Journal of Inorganic Biochemistry 192 (2019) 17–24

Contents lists available at ScienceDirect

Journal of Inorganic Biochemistry

journal homepage: www.elsevier.com/locate/jinorgbio

Synthesis, characterization, DNA binding, topoisomerase I inhibition and antiproliferation activities of three new functionalized terpyridine platinum (II) complexes

Keke Chai[a], Wenhua Kuang[b], Zhou Lan[a], Li Zhang[a], Yihui Jiang[a], Tianzhi Han[a], Junlong Niu[a], Jintao Wang[a,*], Xuemin Duan[a,*]

[a] Jiangxi Provincial Key Laboratory of Drug Design and Evaluation, School of Pharmacy, Jiangxi Science & Technology Normal University, Nanchang 330013, PR China
[b] School of Life Sciences, Tsinghua University, Beijing 100010, PR China

ARTICLE INFO

Keywords:
Platinum complexes
Cytotoxicity
DNA binding
Topoisomerase I inhibition

ABSTRACT

Three new platinum(II) complexes with pendent morpholine were synthesized, namely complex **1** ([Pt(L)Cl]CF_3SO_3), complex **2** ([Pt(L)(NH_3)]$(CF_3SO_3)_2$) and complex **3** ([Pt(L)(PPh_3)]$(CF_3SO_3)_2$), where L = 4′-[4-(4-morpholinobutyloxy)phenyl]-2,2′:6′,2″-terpyridine and PPh_3 = triphenylphosphine. The detailed molecular structures of complex **3**, L and its precursor L′ (1,4′-[4-(4-bromobutyloxy)phenyl]-2,2′:6′,2″-terpyridine) were determined by single crystal X-ray diffraction. An evaluation of in vitro cytotoxicity for both ligand and complexes was performed by methyl thiazolyl tetrazolium (MTT) assay in three cancer cell lines and normal cells as the control, respectively. IC_{50} values of complexes **1–3** were lower than those exhibited for the reference drug cisplatin, and selectivity of these complexes were greater than cisplatin. Among them, complex **3** with a leaving group PPh_3 was found to be the most efficacious complex against certain cell lines, especially for cisplatin-resistant A549cisR cells. These complexes were found to bind DNA, induce efficient DNA unwinding. Meanwhile, topoisomerase (Topo) I inhibitory activities by three complexes were detected, and a minimum inhibitory concentration of 15 μM of complex **3** was found totally inhibit Topo I activity.

1. Introduction

Topoisomerase (Topo) I is a nuclear enzyme and the main role of which is to resolve DNA supercoiling of chromosomes during DNA replication and transcription in both prokaryotes and eukaryotes cells [1,2]. This enzyme is overexpressed in cancer cells, hence, Topo I inhibition is an extremely good method in cancer therapy because it can give rise to DNA damage that induces apoptosis and necrosis, thereby stopping DNA replication [3,4]. Some crucial clinically used antitumor topoisomerase I inhibitors, such as irinotecan [5] and topotecan [6], are called topoisomerase I poisons and their mechanism of action and role in the anticancer activity has been widely discussed. Functionalized terpyridine derivatives [7–10] have a wide range of potential applications ranging from colorimetric metal determination to DNA binding agents, anticancer agents and topoisomerase inhibitors. Interaction with DNA appears to allow terpyridine complexes to combine cytotoxicity with antiviral properties [11]. Square planar platinum(II) intercalators, consisting of terpyridine or its derivatives and a monodentate ligand in the remaining position, have attracted much interest in recent years due to their biological activity, which includes remarkable in vitro cytotoxicity against various cancer cell lines, exceeding that of cisplatin in some cases [12].

Studies on the DNA interaction properties of such complexes are a major goal of bioinorganic chemistry because it can provide fundamental information for developing DNA structural probes and potential biological and therapeutic applications, as well as a better understanding of the mechanism of drug action [13,14]. There is growing interest in exploring the DNA binding mode of metal complexes to assist the rational design and construction of new and efficient drugs targeting DNA [15]. Small molecules interact with double-helical DNA in a noncovalent manner through three binding modes: electrostatic interaction, groove binding and intercalative binding [16]. Among these, the most effective is intercalative binding, which is directly related to antitumor activity [17,18].

In the present study, in order to optimise the biological activity of Pt (II) complexes, we designed and synthesized a terpyridine ligand modified with morpholine derivatives (Scheme 1). Morpholine and its derivatives have interesting biological and pharmacological properties

* Corresponding authors.
E-mail addresses: jintaochem@163.com (J. Wang), duanxuemin@126.com (X. Duan).

https://doi.org/10.1016/j.jinorgbio.2018.12.003
Received 19 July 2018; Received in revised form 27 November 2018; Accepted 2 December 2018
Available online 07 December 2018
0162-0134/

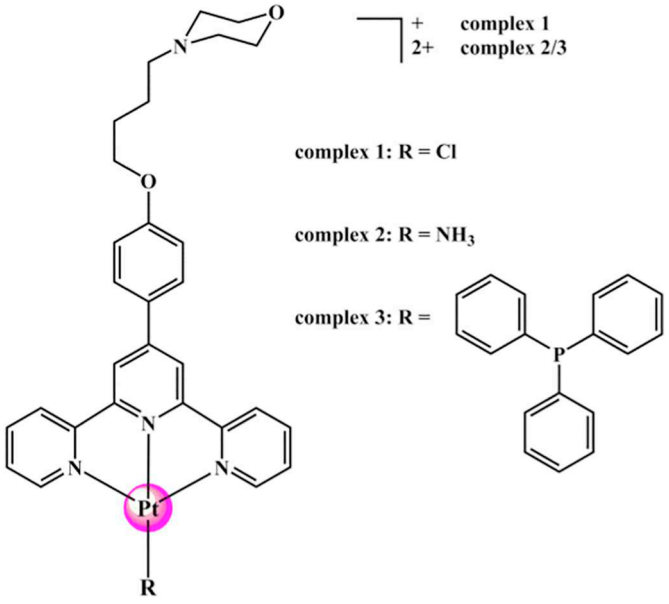

Scheme 1. Molecular structure of the Pt(II) complexes **1–3**.

such as anticancer [19], antiinflammatory, antioxidant and tyrosinase inhibitory activities, and are used in photodynamic therapy [20]. 4-Phenyl-morpholine derivatives also show antimicrobial, antiinflammatory and central nervous system activities [21]. The nitrogen of morpholine is an electron donor that facilitates intermolecular hydrogen bonding [22]. Complexes featuring a chloride co-ligand decompose in aqueous media, but replacing the chloride ligand with 1,3,5-triaza-7-phoshatricyclo[3.3.1.1]decane or triphenylphosphine (PPh_3) results in highly stable, positively charged compounds that exhibit antiproliferative activity dependent on the lipophilicity of the P-based co-ligand [23]. Another reported mitochondrion-targeting Cu(II) complex with introduced PPh_3 group exhibited potent cytotoxicity against cisplatin-resistant tumor cells through multiple mechanisms of action [24]. Herein, three leaving groups, Cl^-, NH_3 and PPh_3, were used to build the complexes **1–3**. DNA binding, topoisomerase I inhibition and cytotoxicity against tumor cells of those morpholino-phenol-substituted platinum(II) complexes were also studied.

2. Experimental section

2.1. Materials and methods

All reagents and materials were purchased from commercial suppliers which for scientific laboratory. 2-Acetylpyridine, *p*-hydroxybenzaldehyde, morpholine, 1,4-dibromobutane, K_2PtCl_4 and triphenylphosphine (PPh_3) were purchased from Energy-chemical. 4′-(4-Hydroxyphenyl)-2,2′:6′,2″-terpyridine was prepared according to the published procedure [25]. Calf thymus DNA (CT DNA) was purchased from Sigma-Aldrich. pBR322 DNA was obtained from BBI LIFE SCIENCES and GelRed was purchased from Biotium. Topoisomerase (Topo I) was obtained from Takara Biomedical Technology (Beijing). Agarose gel, ethylenediaminetetraacetic acid (EDTA) and Tris buffer reagents were purchased from Sangon. A549 (human lung carcinoma cell lines), *cis*platin-resistant A549 (A549cisR), HepG2 (human liver hepatocellular carcinoma), and LO2 (human normal liver cell) were obtained from the Cell Resource Center, Peking Union Medical College (Beijing, China).

Nuclear magnetic spectra were recorded on a Bruker AVANCE 400 spectrometer under ambient condition. Elemental analyses of C, H and N were measured on a Perkin-Elmer 240C elemental analyzer. High resolution mass spectrometric analysis was carried out on a Waters Xevo G2-XS Q-TOF instrument. A Shimadzu UV-2550 UV–vis spectrophotometer was used for UV scanning. Bio-Rad Sub-Cell GT electrophoresis system was used for the electrophoresis experiment and JUNYI scanner (JY04s-3c) was used for gel imaging. Stock solutions (10 mM) of both complexes were prepared in DMSO, which were further diluted using buffer or cell culture medium until working concentrations were achieved.

2.2. Synthesis

2.2.1. L′ (1.4′-[4-(4-bromobutyloxy)phenyl]-2,2′:6′,2″-terpyridine)

The L′ was synthesized according to previously reported method [26] with slight modifications. 1,4-Dibrombutane (3.6 mL, 30 mmol) was added to the solution containing 4′-(4-hydroxyphenyl)-2,2′:6′,2″-terpyridine (1.95 g, 6 mmol) and potassium carbonate (1.65 g, 12 mmol) in 150 mL DMF. After the resulting mixture was heated at 85 °C for 24 h, 50 mL $CHCl_3$ was added. Then the resulting mixture was washed by saturated NaCl aqueous solution (3 × 50 mL), and the combined organic fraction was dehydrated by $MgSO_4$. After filtration, the solvent was removed by reduced pressure distillation. The residue was dissolved in 20 mL of ethyl acetate and the resulting solution was stirring kept overnight. The precipitate was filtered off and was washed with 10 mL diethyl ether. It was dried under vacuum to give 1.62 g the ivory powder. Yield: 58.7%. All characterization data matched that previously reported [21].

2.2.2. L (4′-[4-(4-morpholinobutyloxy)phenyl]-2,2′:6′,2″-terpyridine)

L′ (1.08 g, 2.4 mmol) was dissolved in DMF (45 mL) containing triethylamine (6 mL), followed by adding morpholine (0.08 g, 6 mmol) and the reaction mixture was heated at 155 °C for 1 h. After cooling to room temperature, the resulting solution was poured into sodium chloride saturated aqueous solution (10 mL), and extracted with chloroform (3 × 10 mL). The combined organic layers were washed with H_2O (3 × 10 mL) and dried over $MgSO_4$. After evaporating the solvent under reduced pressure, the residue was purified by flash chromatography on silica gel to give a pale yellow powder. It was dried under vacuum to give 0.78 g the pale yellow powder. Yield: 85%. ^{1}H NMR (400 MHz, $CDCl_3$, δ, ppm): 8.91 (m, 6H, 4, 7, 9, 12 and 1, 15-tpyH), 8.55 (d, 2H, 3, 13-tpyH), 8.20 (d, 2H, 17, 21-tpyH), 7.91 (d, 2H, 2, 14-tpyH), 7.22(d, 2H, 18, 20-tpyH), 4.16 (t, 2H, H22), 3.58 (t, 4H, H27, 28), 2.35 (m, 6H, H25, 26, 29), 1.79 (m, 2H, H23), 1.62 (m, 2H, H24). ^{13}C NMR (400 MHz, $CDCl_3$, δ, ppm): 159.84, 156.57, 155.68, 149.92, 149.26, 136.99, 130.85, 128.68, 123.90, 121.51, 118.41, 114.99, 67.87, 66.87, 58.70, 53.73, 27.29, 23.04. HR–MS (Acetonitrile) *m/z*: calcd 467.2447 for $C_{29}H_{31}N_4O_2$, found 467.2441 for $[L + H]^+$. Elemental analysis calcd (%) for $C_{29}H_{30}N_4O_2$: C 74.65, H 6.48, N 12.01; found: C 74.43, H 6.72, N 12.22.

2.2.3. Complex 1 ([Pt(L)Cl]CF_3SO_3)

A mixture containing $Pt(DMSO)_2Cl_2$ (0.422 g, 1.00 mmol) [27] and 1 equivalent of L (0.466 g, 1.00 mmol) in 40 mL of trichloromethane was reflux under argon for 24 h. The reaction mixture was then cooled to room temperature and the resulting yellow precipitate was filtered off, washed with 10 mL chloroform and 10 mL diethyl ether. The residue was dissolved in 20 mL DMF, and 5 equivalent of KCF_3SO_3 aqueous solution was added. Yellow precipitates were produced immediately, which were collected and dried under vacuum to give 0.58 g yellow powder. Yield: 83%. ^{1}H NMR (400 MHz, DMSO-d_6, δ, ppm): 8.76–8.84 (m, 6H, 4, 7, 9, 12 and 1, 15-tpyH), 8.47 (d, 2H, 3, 13-tpyH), 8.18 (d, 2H, 17, 21-tpyH), 7.86 (d, 2H, 2, 14-tpyH), 7.19 (d, 2H, 18, 20-tpyH), 4.17 (t, 2H, H22), 3.72 (m, 4H, H27, 28), 2.89 (s, 2H), 2.73 (s, 2H), 1.82 (m, 4H, H23, 24). ^{13}C NMR (400 MHz, DMSO-d_6, δ, ppm): 161.78, 158.18, 154.08, 151.86, 150.72, 142.14, 129.75, 128.82, 126.34, 125.42, 120.03, 115.05, 67.65, 65.36, 57.05, 52.76, 26.29, 21.78. HR–MS (Acetonitrile) *m/z*: calcd 696.1705 for $C_{29}H_{30}ClN_4O_2Pt$, found 696.1700 for [**1** - CF_3SO_3]$^+$. Elemental analysis calcd (%) for

$C_{30}H_{30}ClF_3N_4O_5PtS$: C 42.58, H 3.57, N 6.62; found: C 42.43, H 3.73, N 6.41.

2.2.4. Complex 2 ([Pt(L)(NH$_3$)](CF$_3$SO$_3$)$_2$)

A solution of complex **1** (0.169 g, 0.20 mmol) and $AgNO_3$ (0.068 g, 0.4 mmol) in DMF was heated at 80 °C under mixing for 24 h in dark. The resulting AgCl precipitate was filtered, and 12 mL 35% ammonia solution was added to the DMF filtrate. A clear deep yellow solution was obtained and stirred for another 6 h. Then 5 equivalent of KCF_3SO_3 was added and a dull yellow solid was obtained. The resulting precipitate was filtered off, washed with 10 mL diethyl ether. It was dried under vacuum to give 0.13 g brown powder. Yield: 66.7%. ^{1}H NMR (400 MHz, DMSO-d_6, δ, ppm): 8.89–8.95 (m, 6H, 4, 7, 9, 12 and 1, 15-tpyH), 8.59 (d, 2H, 3, 13-tpyH), 8.20 (d, 2H, 17, 21-tpyH), 8.01 (d, 2H, 2, 14-tpyH), 7.23 (d, 2H, 18, 20-tpyH), 5.59 (s, 3H, NH), 4.16 (t, 3H), 2.36 (m, 6H), 1.79 (m, 2H, H_{23}), 1.63 (m, 2H, H_{24}). ^{13}C NMR (400 MHz, DMSO-d_6, δ, ppm): 161.77, 158.26, 154.36, 152.33, 142.71, 129.59, 128.77, 126.20, 122.18, 120.21, 114.97, 68.05, 66.07, 57.56, 53.49, 26.20, 22.05. HR–MS (Acetonitrile) *m/z*: calcd 339.1141 for $[C_{29}H_{33}N_5O_2Pt]^{2+}$, found 339.1143 for [**2** - $2CF_3SO_3]^{2+}$. Elemental analysis calcd (%) for $C_{31}H_{33}F_6N_5O_8PtS_2$: C 38.12, H 3.41, N 7.16; found: C 37.96, H 3.58, N 6.95.

2.2.5. Complex 3 ([Pt(L)(PPh$_3$)](CF$_3$SO$_3$)$_2$)

The complex **3** was synthesized according to similar previously reported method [28] Complex **1** (0.169 g, 0.20 mmol) and $AgCF_3SO_3$ (0.256 g, 1.00 mmol) were added into a dry flask containing 30 mL anhydrous acetonitrile. After refluxing for 46 h, AgCl was filtered off. PPh_3 (0.052 g, 0.2 mmol) was added to the residue, and the solution was stirred for 24 h. Then the resulting precipitate was filtered, washed with 10 mL diethyl ether. It was dried under vacuum to give 0.19 g deep powder. Yield: 77.7%. ^{1}H NMR (400 MHz, DMSO-d_6, δ, ppm): 9.15 (t, 2H, 7, 9-tpyH), 8.97 (t, 2H, 4, 12-tpyH), 8.47 (t, 2H, 1, 15-tpyH), 8.33 (t, 2H, 3, 13-tpyH), 8.17 (m, 5H, PPh_3H), 7.75 (d, 2H, 18, 20-tpyH), 7.67 (m, 5H, PPh_3H), 7.53 (d, 2H, 18, 20-tpyH), 7.37 (m, 5H, PPh_3H), 7.27 (d, 2H, 18, 20-tpyH), 4.19 (t, 2H, H_{27}), 4.01 (t, 2H, H_{28}), 3.65 (m, 3H), 3.22 (t, 2H, H_{26}), 3.08 (t, 2H, H_{29}), 1.85 (m, 5H). ^{13}C NMR (400 MHz, DMSO-d_6, δ, ppm): 162.06, 159.80, 154.51, 153.65, 152.98, 143.77, 135.15, 133.37, 130.00, 128.62, 126.37, 125.80, 124.76, 120.25, 115.33, 67.69, 63.39, 56.07, 51.51, 25.98, 20.29. HR–MS (Acetonitrile) *m/z*: calcd 461.6464 for $[C_{47}H_{45}N_4O_2PPt]^{2+}$, found 461.6459 for [**3** - $2CF_3SO_3]^{2+}$. Elemental analysis calcd (%) for $C_{49}H_{45}F_6N_4O_8PPtS_2$: C 48.16, H 3.71, N 4.58; found: C 48.51, H 4.34, N 4.41.

2.3. Single crystal X-ray data collection and structure refinement

The diffraction data were collected using an Agilent Gemini EOS diffractometer with graphite-monochromated with Mo-Kα radiation (λ = 0.71073 Å) at 293 K for L′ (0.38 × 0.28 × 0.17 mm), 298 K for L (0.42 × 0.31 × 0.16 mm) and 293 K for complex **3** (0.20 × 0.15 × 0.11 mm). An empirical absorption correction was applied. All the non-hydrogen atoms were refined anisotropically and the hydrogen atoms of organic molecule were refined in calculated positions, assigned isotropic thermal parameters, and allowed to ride their parent atoms. All calculations were performed using the *SHELX2014* program package [29]. Crystallographic data (excluding structure factors) for the structures reported in this paper have been deposited in the Cambridge Crystallographic Data Centre with the reference numbers 1851369 for L, 1851370 for L′ and 1851371 for complex **3**.

2.4. DNA binding experiments

2.4.1. UV/Vis absorption titration

Absorption spectra were recorded on a UV/Vis spectrophotometer. A pH 7.4 phosphate-buffered saline (PBS) buffer was used and UV/Vis spectra were recorded after each addition of concentrated DNA stock to 50 μM Pt(II) complex solutions in a quartz cuvette (path length = 1 cm) at 25 °C. Binding data was determined with equation [30,31].

$$[DNA]/(\varepsilon_A - \varepsilon_f) = [DNA]/(\varepsilon_b - \varepsilon_f) + 1/(K_b(\varepsilon_b - \varepsilon_f))$$

where [DNA] is the concentration of DNA in base pairs, $\varepsilon_A = A_{obs}/$[compound], ε_f = the extinction coefficient for the free compound and ε_b = the extinction coefficients for the compound in the fully bound form.

2.4.2. Fluorescence DNA titration

The competitive binding of the tested complexes to CT DNA was determined with ethidium bromide (EB) displacement assay. The CT DNA-EB (20 μM EB, 26 μM CT DNA) conjugation was prepared in PBS buffer. By adding various concentrations of complex solution stepwise, the constants (K_{sv}, M^{-1}) have been calculated and the quenching efficiency for each compound was evaluated according to the classical Stern-Volmer equation [32].

$$I_0/I = 1 + K_{sv}[Q]$$

where I_0 and I are the fluorescence intensities of CT DNA solution in the absence and presence of quencher, [Q] is the concentration of quencher (complexes **1–3** or ligand) and K_{sv} is the Stern-Volmer constant.

2.5. DNA unwinding study

A standard DNA binding assay was used to investigate the effect of complex on the structural of plasmid by agarose gel electrophoresis. DNA unwinding under various concentrations of **1–3** was determined in buffer (10 mM KH_2PO_4, 10 mM NaCl, 10 mM EDTA, pH 7.2). Briefly, after incubation of pBR322 DNA (19 μM base pair concentrations) with complex of different concentrations for 24 h, loading buffer (0.05% bromophenol blue, 50% glycerol, and 2 mM EDTA) was added to the mixture. Then the samples were loaded onto a 0.8% agarose gel and electrophoresed in TBE (1 ×) buffer (89 mM Tris-borate, 2 mM EDTA) at a constant voltage of 120 mV for 80 min. The gels were visualized in the electrophoresis gel documentation and analysis system. The assay of ionic strength dependence of the plasmid DNA unwinding by platinum complex was carried out at 37 °C for 24 h in a pH 7.2, 10 mM KH_2PO_4 buffer. The mixtures contain various concentrations of NaCl aqueous solution (0–200 mM) and pBR322 DNA (19 μM). After incubation for 24 h, loading buffer was added. The gels were visualized in the electrophoresis gel documentation and analysis system.

2.6. Topoisomerase I inhibition assay

Inhibition assay provides a direct method of determining whether the complex affects the activity of Topo I [20]. In the experimental process, a reaction mixture (20 μL) containing 19 μM (base pair concentrations) pBR322 in buffer (10 mM Tris-HCl, 50 mM KCl, 5 mM $MgCl_2$, 0.1 mM DTT, 0.1 mM EDTA, 150 μg/mL BSA, pH 7.5) was incubated with 1 unit Topo I in the absence or in the presence of complex **1** (1–100 μM), **2** (1–40 μM) and **3** (1–15 μM), for 30 min at 37 °C. Each sample was preincubated for 15 min prior to the addition of pBR322 DNA. Loading buffer (0.2% bromophenol blue, 30% glycerol, 4.5% SDS, 0.2% xylene cyanol) was added to the reaction mixture. The image was visualized using analysis system.

2.7. Cytotoxicity test

A standard methyl thiazolyl tetrazolium (MTT) assay was employed to evaluate the potential cytotoxicities of L and three complexes against A549, A549cisR, HepG2 and LO2 cell lines. The cells were maintained in Dulbecco's Modified Eagle's Medium (DMEM) supplemented with 10% FBS 100 μg mL^{-1} streptomycin, and 100 U mL^{-1} penicillin. The

cells were cultured in a humidified incubator, which provided an atmosphere of 5% CO_2 and 95% air at a constant temperature of 37 °C. A549cisR cells were cultured in a medium containing cisplatin to maintain the resistance. In a typical experiment, the cells were seeded in a 96-well flat-bottomed microplate at 10,000 cell per well in growth medium solution. The microplate was incubated at 37 °C with 5% CO_2 in a humidified incubator for 24 h. The medium was then changed to growth medium with or without complexes with serial concentrations. The microplate was then incubated at 37 °C with 5% CO_2 in a humidified incubator for 48 h. After 48 h, MTT (20 μL, 5 mg/mL) was added to each well. The microplate was reincubated at 37 °C in 5% CO_2 for another 4 h. Then the medium was carried out and 150 μL DMSO was added into each well, the microplates were shaken for 10 min. The absorbance at the wavelength of 570 nm was measured by a microplate reader (reference wavelength: 630 nm). The IC_{50} value of each complex (the concentration that is required to reduce the absorbance by 50% relatively to the controls) was analysed and calculated by SPSS.

3. Results and discussion

3.1. Synthesis and characterization

All ligands and complexes were prepared following the procedure shown in Fig. S1, and characterized by elemental analysis, ^{1}H NMR, ^{13}C NMR spectra along with HR-MS spectrometry. White crystals of L′ and L suitable for X-ray diffraction studies were obtained by slow evaporation of acetone solutions, while, yellow crystals of complex **3** was also separated out from a acetonitrile solution. Information concerning X-ray data collection and crystal structure refinement is summarized in Table 1, with the selected bond lengths and bond angles listed in Table S1. The structures are shown in Figs. 1–3 respectively, that prove those products ligands and complexes have the expected molecular.

As shown in Figs. 2 and 3, L′ and L are planar structures, and the obtained bond lengths and bond angles are similar to a reported terpyridine derivative 4-([2,2′:6′,2″-terpyridine]-4′-yl)-*N*,*N*-diethylaniline [12]. The crystal structure shows that complex 3 is a classical four-coordinate Pt(II) complex, in which the Pt is bounded to three N atoms from the chelating ligand terpy and one P atom from PPh_3. In complex

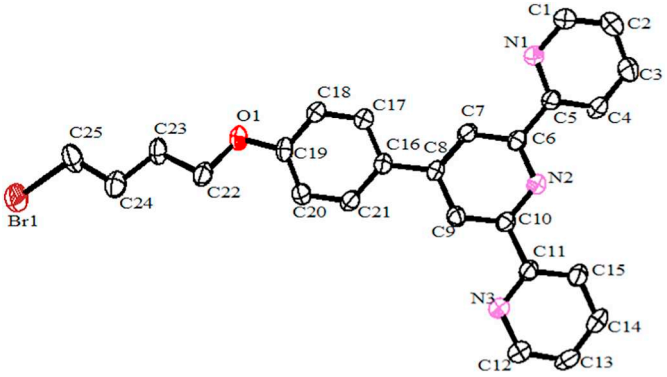

Fig. 1. Thermal ellipsoid plot of L′ in ORTEP view.

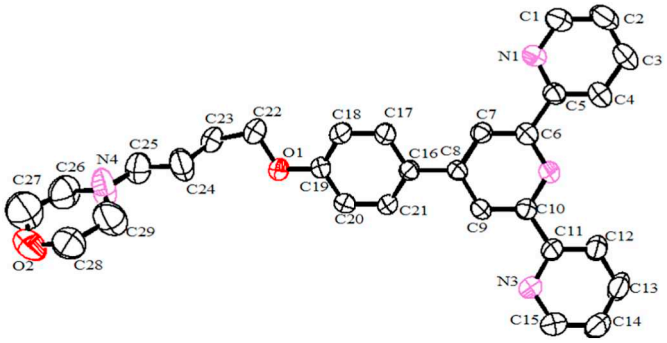

Fig. 2. Thermal ellipsoid plot of L in ORTEP view.

3, the angles among the four coordination bonds (104.0(3) for N1-Pt-P1, 79.8(4) for N1-Pt-N2, 79.2(3) for N2-Pt-N3 and 96.9(2) for N3-Pt-P) sum to 359.9°, confirming the planar geometry. Specifically, the bond angle of and the bond length of 3 are similar compare with the crystal from previously reported [28]. Two $CF_3SO_3^-$ anions are systematically located above and below the Pt-terpy plane, which prevent the π-π stacking interactions between two monomers (Fig. S2).

Table 1
Crystal and structure refinement data for L′, L and complex **3**.

	L′	L	**3**
Chemical formula	$C_{25}H_{22}BrN_3O$	$C_{29}H_{29}N_4O_2$	$C_{49}H_{45}F_6N_4O_8PPtS_2$
Formular weight (g mol^{-1})	460.36	465.56	1222.07
Crystal system	Monoclinic	Monoclinic	Triclinic
Space group	*P* 1 21/*n* 1	*P* 1 21/*C* 1	*P*-1
a (Å)	6.2345 (5)	19.8548 (19)	11.9258 (8)
b (Å)	35.276 (3)	11.6986 (11)	14.8207 (13)
c (Å)	9.6339 (8)	10.8633 (10)	17.5516 (13)
α (°)	90	90	94.774 (7)
β (°)	92.794 (7)	93.535 (7)	103.042 (7)
γ (°)	90	90	111.666 (7)
V (Å^3)	2116.2 (3)	2518.5 (4)	2760.8 (4)
Z	4	4	2
D_c (g cm^{-3})	1.445	1.228	1.470
θ range (°)	3.9650–21.5910	3.1970–21.7670	2.529–26.499
μ (mm^{-1})	0.71073	0.71073	0.710
F (000)	944	988	1220
Crystal size (mm)	0.38 × 0.28 × 0.17	0.42 × 0.31 × 0.16	0.20 × 0.15 × 0.11
Temperature (K)	293 (2)	298.3 (2)	293 (2)
Reflections collected	16,457	11,720	19,156
Independent reflections	2279	2037	5501
Goodness-of-fit (GOF)	1.039	1.023	0.972
Largest difference in peak and hole (e Å^{-3})	0.468, –0.480	0.543, –0.398	1.557, –0.989
R_1[a] wR_2[b] ($I > 2\sigma(I)$)	0.1701, 0.1315	0.1951, 0.3131	0.1768, 0.1689
R_2[a] wR_2[b] (all data)	0.0745, 0.1050	0.0934, 0.2349	0.0918, 0.1323

[a] $R_1 = \Sigma\|F_o| - |F_c\| / \Sigma|F_o|$.
[b] $wR_2 = |\Sigma w(|F_o|^2 - |F_c|^2) / \Sigma|w(F_o)^2|^{1/2}$, where $w = 1 / [\sigma^2(F_o^2) + (aP)^2 + bP]$. $P = (F_o^2 + 2F_c^2) / 3$.

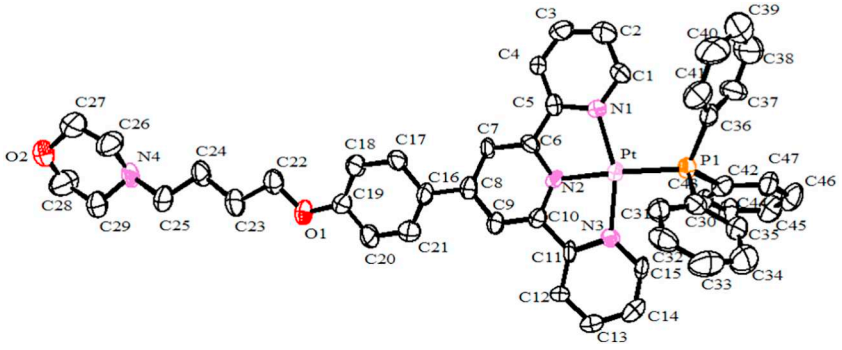

Fig. 3. Thermal ellipsoid plot of complex **3** in ORTEP view.

3.2. DNA binding

The interaction mode of metal complexes with double-stranded DNA is mainly dependent on the structure of the complexes and the nature of their ligands [33]. The existence of labile ligands may lead to their displacement and replacement by a nitrogen atom of a DNA base, resulting in covalent binding of the metal to DNA. As in the case of cisplatin, after the aquation of the one or two chloride ion, platinum(II) is able to coordinate to the nitrogen atoms of the DNA bases. Complexes that remain stable in solution may either induce unwinding of the DNA double helix or engage in non-covalent interactions with DNA, such as $\pi \rightarrow \pi$ stacking interactions of planar aromatic rings of the complex with DNA bases, electrostatic interactions due to the development of coulomb forces towards the DNA phosphate groups, or groove binding arising from the existence of hydrophobic, hydrogen bonding or *van der Waals* forces [34].

Firstly, the interactions of complexes **1–3** with calf thymus DNA (CT DNA) were measured by UV–vis spectroscopy. In this study, interactions can be revealed by the band changes induced by titration of CT DNA. Since both Pt(II) complexes contain the MLCT (MLCT = metal to ligand charge transfer) bands from the terpy ligands, alteration in the UV–vis absorption intensity and wavelength of MLCT bands could provide a measure of the potential binding ability. Herein, the new ligand L was not involved because the MLCT band was unobserved. UV titration spectra of complexes **1–3** with increasing concentrations of CT DNA are shown in Fig. S3, and the calculated binding constants and related parameters are listed in Table 2. Notably, the titration results revealed apparent hypochromism of the MLCT bands of complexes upon the addition of CT DNA. Meanwhile, obvious bathochromic shift was also observed for complex **2**. These shifts are due to the intercalation of the complex, usually involving a strong π-π stacking interaction between an aromatic chromophore and the base pairs of DNA. The DNA binding constants (K_b, Table 2) of complexes were determined from the Wolfe-Shimer equation [35]. However, the K_b constant of L did not include here account for L excludes the MLCT band that was unobserved. The obtained K_b constants of complexes **1–3** were higher than that of the classical intercalator ethidium bromide (EB, $1.4 \times 10^6\ M^{-1}$) as previously calculated [36], and complex **2** exhibited the highest K_b constant among the complexes. With an amino group that could be beneficial to the formation of hydrogen bonds, di-positive charged complex **2** shows better binding ability towards CT DNA.

Secondly, competitive DNA-binding studies with EB were also used to reveal the binding abilities between compounds and CT DNA. The fluorescence emission spectra of the prepared EB-DNA system in the presence of increasing amounts of complexes **1–3** of different ratios of r (r = [compound] / [DNA]) were recorded. As shown in Fig. S4, the addition of L or complexes **1–3** at diverse concentrations induced a dramatic decrease of the fluorescence intensity of the emission band from the CT DNA-EB system. The Stern-Volmer plot of DNA-EB (Fig. S5) illustrates that the quenching of EB bound to DNA by these compounds, resulting in a decrease in the fluorescence intensity. Obviously, the calculated K_{sv} values of L is lowest, and complex **2** bearing the highest K_{sv} ($8.49 \times 10^4\ M^{-1}$) values (Table 3). Meanwhile, the results obtained here are consistent well with UV–vis titration data. Herein the effectively quenching of fluorescence of DNA-EB system by complexes **1–3** suggesting that they can interact with CT DNA via the intercalative mode, and EB was replaced from DNA-EB conjugation [33].

3.3. DNA unwinding activity studies

The DNA unwinding can be defined by the ability of metal complexes to convert the closed supercoiled circular from of the DNA (Form I) to the open circular relaxed form (Form II) or the linear form (Form III) [37,38]. Experiments with different concentrations of the platinum (II) complex were conducted in a pH 7.2 buffer (10 mM KH_2PO_4, 10 mM NaCl, 10 mM EDTA). The results show that the Pt(II) complex acted as a chemical nuclease by unwinding DNA from Form I into Form II (Fig. 4). With an increasing concentration of the Pt(II) complex, Form I gradually diminished accompanied by the increasing of Form II. Noticeably, the DNA unwinding activities of the Pt(II) complexes were concentration-dependent. When the concentration of complex **1** reached to 8 μM, Form I was converted into Form II completely. Complex **2** and **3** also showed similarly potent DNA unwinding activities. Meanwhile, the ligand L hardly shows unwinding activity against DNA when its concentration increased to 40 μM (Fig. S6). Moreover, the DNA untwisting activity of complex, which similar to the cytotoxicity in the cytostatic mechanism, is positively related to its concentration [24]. Thus, the obviously unwinding ability suggests that the complexes with good potential anticancer activity.

Since the activation of chlorido Pt(II) complexes via hydrolysis

Table 2
The DNA-binding constants (K_b) value of complexes **1–3**.

Complexes	Band ($\Delta A/A_0$[a], $\Delta\lambda$[b])	$K_b(M^{-1})$
1	416 (−32%, +1)	5.23×10^6
2	396 (−25%, +7)	9.57×10^6
3	388 (−10%, 0)	5.27×10^6

[a] "+" denotes hyperchromism, "−" denotes hypochromism.
[b] "+" denotes red-shift, "−" denotes blue-shift.

Table 3
The values of Stern-Volmer constant (K_{sv}) and percentage of fluorescence of L and complexes **1–3**.

Compounds	$\Delta I/I_0$ (%)	K_{sv} (M^{-1})
L	9	4.40×10^3
1	57	7.18×10^4
2	68	8.49×10^4
3	65	8.16×10^4

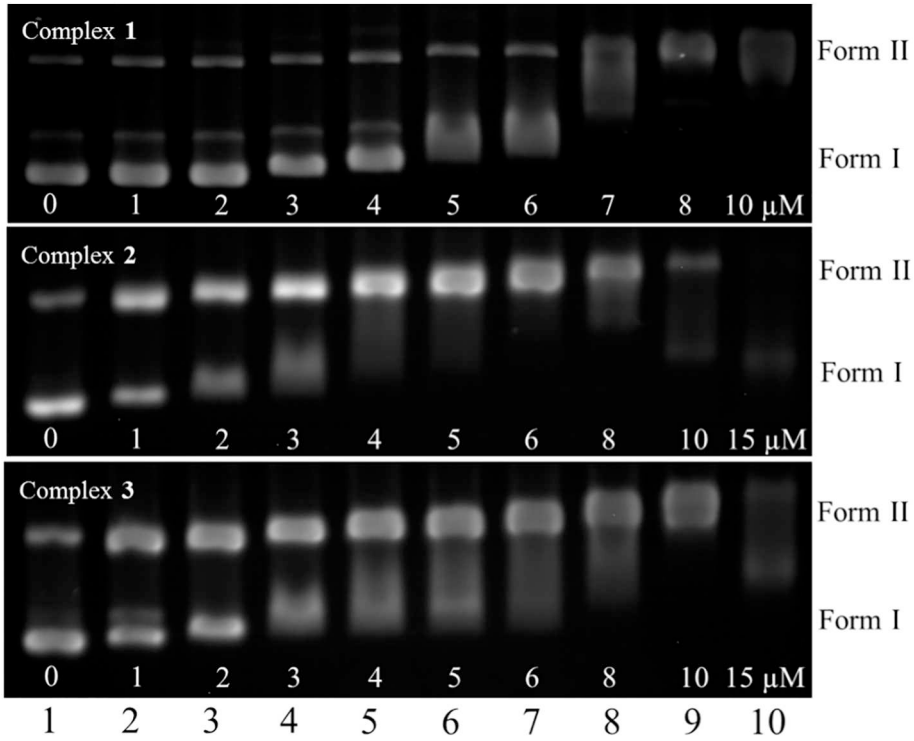

Fig. 4. Concentration-dependent of pBR322 DNA unwound by Pt(II) complexes **1–3** at 37 °C for 24 h. Lane 1, DNA control, lane 2–10, the pBR322 DNA with **1–3** of different concentrations.

pathway is a significant and potential mechanism for DNA targeting, and this process closely related to the concentration of NaCl in vivo [39]. NaCl (0–100 mM) concentrations dependence of the pBR322 DNA unwinding by **1** (5 μM) was proceeded. As shown in Fig. S7, DNA unwinding ability was inhibited with the increased concentrations of sodium chloride. Maximum inhibition occurred at NaCl concentration of 80 mM. The result indicated that process of unwinding DNA by Pt complex is also a DNA-complex chelating process.

3.4. Topoisomerase I inhibition

Topoisomerases are well-established targets in antitumor research, and compounds inhibiting these enzymes are potential antitumor agents [40]. Therefore, the Topoisomerase I-DNA binding assay was used to investigate the effect of complexes on the activity of human Topo I by agarose gel electrophoresis. It provides a direct means of determining whether the complex inhibit the activity of Topo I so that the unwinding of nicked open circular (form II) DNA to a supercoiled (form I) duplex DNA. The inhibitory effect of the Pt(II) complexes **1–3** on Topo I was investigated by unwinding plasmid pBR322. The results (Fig. 5) indicate that with increasing Pt(II) complex concentration, Form II is diminished accompany with Form I is increased. When the concentration of complex **1** reached to 60 μM, Form II was completely converted into Form I, demonstrating that the Pt(II) complex exhibited effectively concentration-dependent Topo I inhibitory activity. Maximum Topo I inhibition was achieved when the concentration of complex **2** or **3** reached to 15 μM. Remarkably, complexes **2** and **3** were more potent Topo I inhibitors than complex **1**. Furthermore, L did not show obvious effect on inhibitory activity to Topo I in control experiments (Fig. S8). The cisplatin, which was taken as reference, exhibited a similar inhibiting effect compared with other reported [41], and its inhibitory effect was not as effective as complexes **1–3** (Fig. S9). In summary, the Pt(II) complexes described herein possess potent concentration-dependent Topo I inhibitory activity and prevent enzyme-mediated unwinding of supercoiled pBR322 plasmid DNA. In general, the ability of antiproliferation on the cancer cells is in accordance with the capacity of the catalytic activity of Topo I to DNA [42]. Thus, the metal-based complexes as efficient topoisomerase I inhibitors could be expected to show high antitumor activities.

3.5. In vitro anticancer activity

The cytotoxicities of the complexes against A549, A549cisR, and HepG2 cancer cell lines were determined by MTT assays. Their toxicity to normal cells was also explored on the human normal liver LO2 cell line under the same conditions. Cisplatin was used as a positive control in these studies. The resulting IC_{50} values are given in Table 4. Based on these values, the in vitro antiproliferative activities of the compounds follow the order: **3** > **2** > **1** > cisplatin > L. Complex **3**, with IC_{50} values ranging from 2.9 to 8.2 μM, show much higher cytotoxicity than complexes **1**, **2**, cisplatin and the ligand against all the human cancer cell lines tested. Meanwhile, Complex **3** is highly cytotoxic against cisplatin-resistant A549cisR cells, indicating they are not cross-resistant with cisplatin. This result indicates that the cytotoxicity of complex **3** towards A549 and A549cisR cells is very similar, and A549cisR cells do not show evident resistance to **3**. Interestingly, a relatively high selectivity towards cancer cells (HepG2) over normal cells (LO2) is observed for complexes **1–3**, showing approximately 5-fold higher cytotoxicity against cancer cell lines tested than that against LO2 cells. The anti-proliferation of L is much lower than **1–3** and cisplatin. In particular, the selectivity indexes (SI) of **3** reveals an interesting value (SI = 16.1) towards A549 line over LO2 cells, 16-fold higher than the cisplatin. Meanwhile, the SI (IC_{50} in A549cisR/IC_{50} in LO2) of **3** is 11.4, which was 5.7-fold higher than that of cisplatin. It has been reported that after the introducing of triphenylphosphine, the ability of acrossing cell membranes or mitochondrial membranes was enhanced [19]. Herein the best anti-proliferation of **3** might result from the strong lipophilic capability in itself. Furthermore, its cell selectivity was enhanced might due to the introduced morphine moiety, which as an excellent pharmacophore because it possessing unique hydrogen bonds

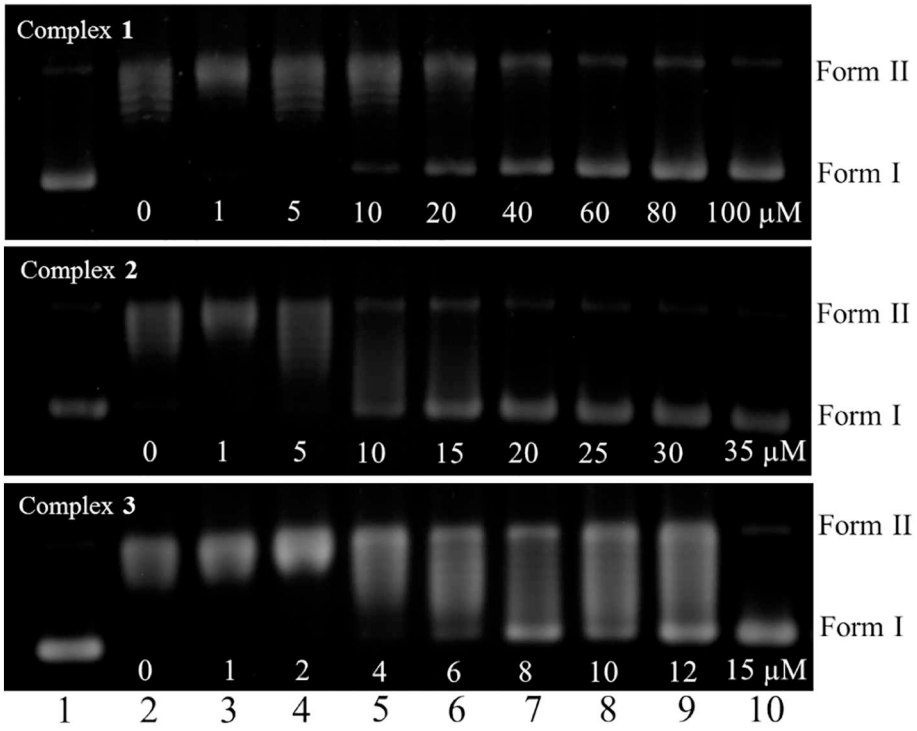

Fig. 5. Concentration-dependent of Topo I inhibitory effect by **1–3**. Lane 1, DNA control, lane 2–10, Topo I + **1–3** of different concentrations.

Table 4
IC_{50} values of L and complexes **1–3** towards different cell lines.[a]

Compound	IC_{50} [μM]			
	A549	A549cisR	HepG2	LO2
L	32.7 ± 5.1	45.2 ± 5.2	50.1 ± 6.3	89.7 ± 5.9
1	8.3 ± 1.0	15.6 ± 2.1	15.5 ± 1.2	79.8 ± 7.1
2	7.9 ± 0.8	9.1 ± 0.7	8.3 ± 0.7	69.7 ± 5.6
3	2.9 ± 0.4	4.1 ± 0.5	8.2 ± 0.8	46.6 ± 8.1
Cisplatin	16.1 ± 1.9	59.3 ± 1.6	12.5 ± 1.8	15.6 ± 2.1

[a] IC_{50} values are drug concentrations necessary for 50% inhibition of cell viability. Data are presented as means ± standard deviations of at least three independent experiments and the drug treatment period was 48 h.

in biological system [43]. Meanwhile, the SI = 8.4 is observed for **2** towards HepG2 line over LO2 cells, 6.7 times higher than cisplatin and 4.7 times higher than L. It has been reported that introducing of NH_3 to compound is a useful strategy, which could benefit for the anti-proliferation [44]. From the present results, it may be concluded that **3** appears to be promising agent for further investigation, especially for in vivo studies.

4. Conclusions

In the present work, three Pt(II) complexes bearing morpholine modified terpyridine ligand and different leaving groups, complex **1** ($[Pt(L)Cl]CF_3SO_3$), **2** ($[Pt(L)(NH_3)](CF_3SO_3)_2$) and **3** ($[Pt(L)(PPh_3)](CF_3SO_3)_2$) were synthesized and the detailed structures of L, L′ and complex **3** were confirmed by X-ray crystallography. The crystal structures showed that the Pt(II) center is in a square-planar conformation in complex **3**, and π-π stacking interaction was not detected because the presence of two counter anions $CF_3SO_3^-$ can cause steric effects. The binding abilities between those complexes and CT DNA were investigated and the result showed that the highest calculated DNA-binding constants K_b of complex **2** reach to $9.57 \times 10^6\,M^{-1}$, which exhibited stronger DNA binding affinity than that of the classical DNA intercalator EB and complexes **1/3**. This probably attribute to the stronger intercalary and electrostatic intercalation interaction between DNA and complex **2**. Meanwhile, complexes **1–3** showed significant topoisomerase I inhibitory activity, and complex **2/3** were more potent than complex **1**. Complexes **1–3** achieved significantly anticancer activities against those three cancer cell lines, which were more potent than the drug cisplatin. Importantly, they exhibited remarkable activities against cisplatin-resistant human lung cancer cell lines, suggesting that they performed via a novel mechanism of action. Hence, the role played by DNA interaction or Topoisomerase I inhibition mode of action in cell death induced by these new platinum(II) complexes deserve further investigation in cancer cells for highlighting the potential of those Pt(II) complexes as antitumor agents. Overall, our results suggest that changing the leaving groups in the aromatic Pt(II) coordination plane and introducing suitable bioactive groups could be promising strategies for developing Pt(II) polypyridyl complexes as selective DNA binders and potential anticancer agents.

Abbreviations

PPh_3	triphenylphosphine
Topo I	topoisomerase I
CT DNA	calf thymus DNA
NMR	Nuclear Magnetic Resonance
K_b	DNA binding constants
EB	ethidium bromide
EDTA	ethylenediaminetetraacetic acid
DTT	DL-Dithiothreitol
BSA	bovine serum albumin
DMF	*N*,*N*-dimethylformamide
DMSO	dimethyl sulfoxide
SDS	sodium dodecyl sulphate
SI	selectivity index
MTT	methyl thiazolyl tetrazolium
DMEM	Dulbecco's Modified Eagle's Medium

Acknowledgements

We thank the National Natural Science Foundation of China (21401105), Jiangxi Provincial Key Laboratory of Drug Design and Evaluation (20171BCD40015), Natural Science Foundation of Jiangxi Province (20181BAB213001), Jiangxi Provincial Department of Education (GJJ170695) and the Research Fund for the Doctoral Program of Jiangxi Science & Technology Normal University (3000990404).

Appendix A. Supplementary material

Crystallographic data for the structures in this paper have been deposited with the Cambridge Crystallographic Database Center, CCDC, 12 Union Road, Cambridge CB21EZ, UK. Copies of the data can be obtained free of charge on quoting the deposition numbers CCDC 1851369 for L, 1851370 for L′, 1851371 for complex **3** (Fax: +44-1223-336-033; E-mail: deposit@ccdc.cam.ac.uk). Supplementary data to this article can be found online at https://doi.org/10.1016/j.jinorgbio.2018.12.003.

References

[1] L.F. Liu, Annu. Rev. Biochem. 58 (1989) 351–375.
[2] W.D. Kingsbury, J.C. Boehm, D.R. Jakas, K.G. Holden, S.M. Hecht, G. Gallagher, M.J. Caranfa, F.L. McCabe, L.F. Faucette, R.K. Johnson, J. Med. Chem. 34 (1991) 98–107.
[3] J.L. Nitiss, K.C. Nitiss, A. Rose, J.L. Waltman, J. Biol. Chem. 276 (2001) 26708–26714.
[4] J. Malina, O. Vrana, V. Brabec, Nucleic Acids Res. 37 (2009) 5432–5442.
[5] Y. Pommier, Nat. Rev. Cancer 6 (2006) 789–802.
[6] W. ten Bokkel Huinink, M. Gore, J. Carmichael, A. Gordon, J. Malfetano, I. Hudson, C. Broom, C. Scarabelli, N. Davidson, M. Spanczynski, G. Bolis, H. Malmstrom, R. Coleman, S.C. Fields, J.F. Heron, J. Clin. Oncol. 15 (1997) 2183–2193.
[7] Y. Lo, T. Ko, W. Su, T. Su, A. Wang, J. Inorg. Biochem. 103 (2009) 1082–1092.
[8] H. Kwon, C. Park, K. Jeon, E. Lee, S. Park, K. Jun, T. Kadaya, P. Thapa, R. Karki, Y. Na, M. Park, S. Rho, E. Lee, Y. Kwon, J. Med. Chem. 58 (2015) 1100–1122.
[9] J. Son, L. Zhao, A. Basnet, P. Thapa, R. Karki, Y. Na, Y. Jahng, T. Jeong, B. Jeong, C. Lee, E. Lee, Eur. J. Med. Chem. 43 (2008) 675–682.
[10] L.X. Zhao, T.S. Kim, S.H. Ahn, T.H. Kim, E.K. Kim, W.J. Cho, H. Choi, C.S. Lee, J.A. Kim, T.C. Jeong, C.J. Chang, E.S. Lee, Bioorg. Med. Chem. Lett. 11 (2001) 2659–2662.
[11] J.T. Wang, Y. Li, J.H. Tan, L.N. Ji, Z.W. Mao, Dalton Trans. 40 (2011) 564–566.
[12] H.H. Zou, L. Wang, Z.X. Long, Q.P. Qin, Z.K. Song, T. Xie, S.H. Zhang, Y.C. Liu, B. Lin, Z.F. Chen, Eur. J. Med. Chem. 108 (2016) 1–12.
[13] A.E. Friedman, J.C. Chambron, J.P. Sauvage, N.J. Turro, J.K. Barton, J. Am. Chem. Soc. 112 (1990) 4960–4962.
[14] C. Metcalfe, J.A. Thomas, Chem. Soc. Rev. 32 (2003) 215.
[15] M.L. Yola, N. Özaltın, J. Electroanal. Chem. 653 (2011) 56–60.
[16] Y. Zhang, X. Wang, L. Ding, J. Serb, Chem. Soc. 75 (2010) 1191–1201.
[17] G. Zhang, P. Fu, L. Wang, M. Hu, J. Agric. Food Chem. 59 (2011) 8944–8952.
[18] J. Tan, B. Wang, L. Zhu, Bioorg. Med. Chem. 17 (2009) 614–620.
[19] P. Doan, A. Karjalainen, J.G. Chandraseelan, O. Sandberg, O. Yli-Harja, T. Rosholm, R. Franzen, N.R. Candeias, M. Kandhavelu, Eur. J. Med. Chem. 120 (2016) 296–303.
[20] B. Barut, U. Demirbas, A. Ozel, H. Kantekin, Int. J. Biol. Macromol. 105 (2017) 499–508.
[21] P. Panneerselvam, R.R. Nair, G. Vijayalakshmi, E.H. Subramanian, S.K. Sridhar, Eur. J. Med. Chem. 40 (2005) 225–229.
[22] R.H. Morris, Chem. Rev. 116 (2016) 8588–8654.
[23] S. Parveen, M. Hanif, S. Movassaghi, M.P. Sullivan, M. Kubanik, M.A. Shaheen, T. Söhnel, S.M.F. Jamieson, C.G. Hartinger, Eur. J. Inorg. Chem. 12 (2017) 1721–1727.
[24] W. Zhou, X.Y. Wang, M. Hu, C.C. Zhu, Z.J. Guo, Chem. Sci. 5 (2014) 2761–2770.
[25] O.A. Oyetade, V.O. Nyamori, B.S. Martincigh, S.B. Jonnalagadda, RSC Adv. 6 (2016) 2731–2745.
[26] E.K. Beloglazkina, E.A. Manzheliy, A.A. Moiseeva, O.A. Maloshitskaya, N.V. Zyk, D.A. Skvortsov, I.A. Osterman, P.V. Sergiev, O.A. Dontsova, Y.A. Ivanenkov, M.S. Veselov, A.G. Majouga, Polyhedron 107 (2016) 27–37.
[27] J.H. Price, J.P. Birk, B.B. Wayland, Inorg. Chem. 17 (1978) 2245–2250.
[28] T.M. Pappenfus, J.R. Burney, K.A. McGee, G.G.W. Lee, L.R. Jarvis, D.P. Ekerholm, M. Farah, L.I. Smith, L.M. Hinkle, K.R. Mann, Inorg. Chim. Acta 363 (2010) 3214–3221.
[29] G.M. Sheldrick, Acta Crystallogr. Sect. C: Cryst. Struct. Commun. 71 (2015) 3–8.
[30] C. Kumar, E.H. Asuncion, J. Am. Chem. Soc. 115 (1993) 8547–8553.
[31] F. Rosu, E. De Pauw, L. Guittat, P. Alberti, L. Lacroix, P. Mailliet, J.-F. Riou, J.-L. Mergny, Biochemistry 42 (2003) 10361–10371.
[32] F. Dimiza, F. Perdih, V. Tangoulis, I. Turel, D.P. Kessissoglou, G. Psomas, J. Inorg. Biochem. 105 (2011) 476–489.
[33] A. Tarushi, C. Kakoulidou, C.P. Raptopoulou, V. Psycharis, D.P. Kessissoglou, I. Zoi, A.N. Papadopoulos, G. Psomas, J. Inorg. Biochem. 170 (2017) 85–97.
[34] B.M. Zeglis, V.C. Pierre, J.K. Barton, Chem. Commun. (2007) 4565–4579.
[35] A.M. Pyle, J.P. Rehmann, R. Meshoyrer, C.V. Kumar, N.J. Turro, J.K. Barton, J. Am. Chem. Soc. 111 (1989) 3051–3058.
[36] J.B. LePecq, C. Paoletti, J. Mol. Biol. 27 (1967) 87–106.
[37] C. Icsel, V.T. Yilmaz, Y. Kaya, S. Durmus, M. Sarimahmut, O. Buyukgungor, E. Ulukaya, J. Inorg. Biochem. 152 (2015) 38–52.
[38] S.J. Lippard, Acc. Chem. Res. 11 (1978) 211–217.
[39] A. Nomura, Y. Sugiura, J. Am. Chem. Soc. 126 (2004) 15374–15375.
[40] Y. Pommier, P. Pourquier, Y. Fan, D. Strumberg, Biochim. Biophys. Acta 1400 (1998) 83–105.
[41] M. Fukuda, K. Nishio, F. Kanzawa, H. Ogasawara, T. Ishida, H. Arioka, K. Bojanowski, M. Oka, N. Saijo, Cancer Res. 56 (1996) 789–793.
[42] O. Lavergne, D. Demarquay, C. Bailly, C. Lanco, A. Rolland, M. Huchet, H. Coulomb, N. Muller, N. Baroggi, J. Camara, C. Le Breton, E. Manginot, J.B. Cazaux, D.C.H. Bigg, J. Med. Chem. 43 (2000) 2285–2289.
[43] K.R. Senwar, P. Sharma, T.S. Reddy, M.K. Jeengar, V.L. Nayak, V.G.M. Naidu, A. Kamal, N. Shankaraiah, Eur. J. Med. Chem. 102 (2015) 413–424.
[44] N. Hao, K.W. Jayawardana, X. Chen, M. Yan, ACS Appl. Mater. Interfaces 7 (2015) 1040–1045.